

in semantic segmentation. Indeed, starting from early methods using VGGs [1, 2], to the latest methods with significantly deeper and more powerful backbones [3], the evolution of backbones has dramatically pushed the performance boundary of semantic segmentation. Besides backbone architectures, another line of work formulates semantic segmentation as a structured prediction problem, and focuses on designing modules and operators, which can effectively capture contextual information. A representative example in this area is dilated convolution [4, 5], which increases the receptive field by “inflating” the kernel with holes.

Witnessing the great success in natural language processing (NLP), there has been a recent surge of interest to introduce Transformers to vision tasks. Dosovitskiy et al. [6] proposed vision Transformer (ViT) for image classification. Following the Transformer design in NLP, the authors split an image into multiple linearly embedded patches and feed them into a standard Transformer with positional embeddings (PE), leading to an impressive performance on ImageNet. In semantic segmentation, Zheng et al. [7] proposed SETR to demonstrate the feasibility of using Transformers in this task.

SETR adopts ViT as a backbone and incorporates several CNN decoders to enlarge feature resolution. Despite the good performance, ViT has two important limitations: 1) ViT outputs single-scale low-resolution features instead of multi-scale ones, and 2) it has very high computational cost on large images. To address these limitations, Wang et al. [8] proposed a pyramid vision Transformer (PVT), a natural extension of ViT with pyramid structures for dense prediction. PVT shows considerable improvements over the ResNet counterpart on object detection and semantic segmentation. However, together with other emerging methods such as Swin Transformer [9] and Twins [10], these methods mainly consider the design of the Transformer encoder, neglecting the contribution of the decoder for further improvements.

This paper introduces SegFormer, a cutting-edge Transformer framework for semantic segmentation that jointly considers efficiency, accuracy, and robustness. In contrast to previous methods, our framework redesigns both the encoder and the decoder. The key novelties of our approach are:

- A novel positional-encoding-free and hierarchical Transformer encoder.
- A lightweight All-MLP decoder design that yields a powerful representation without complex and computationally demanding modules.
- As shown in Figure 1, SegFormer sets new a state-of-the-art in terms of efficiency, accuracy and robustness in three publicly available semantic segmentation datasets.

First, the proposed encoder avoids interpolating positional codes when performing inference on images with resolutions different from the training one. As a result, our encoder can easily adapt to arbitrary test resolutions without impacting the performance. In addition, the hierarchical part enables the encoder to generate both high-resolution fine features and low-resolution coarse features, this is in contrast to ViT that can only produce single low-resolution feature maps with fixed resolutions. Second, we propose a lightweight MLP decoder where the key idea is to take advantage of the Transformer-induced features where the attentions of lower layers tend to stay local, whereas the ones of the highest layers are highly non-local. By aggregating the information from different layers, the MLP decoder combines both local and global attention. As a result, we obtain a simple and straightforward decoder that renders powerful representations.

We demonstrate the advantages of SegFormer in terms of model size, run-time, and accuracy on three publicly available datasets: ADE20K, Cityscapes, and COCO-Stuff. On Cityscapes, our lightweight model, SegFormer-B0, without accelerated implementations such as TensorRT, yields 71.9% mIoU at 48 FPS, which, compared to ICNet [11], represents a relative improvement of 60% and 4.2% in latency and performance, respectively. Our largest model, SegFormer-B5, yields 84.0% mIoU, which represents a relative 1.8% mIoU improvement while being $5 \times$ faster than SETR [7]. On ADE20K, this model sets a new state-of-the-art of 51.8% mIoU while being $4 \times$ smaller than SETR. Moreover, our approach is significantly more robust to common corruptions and perturbations than existing methods, therefore being suitable for safety-critical applications. Code will be publicly available.

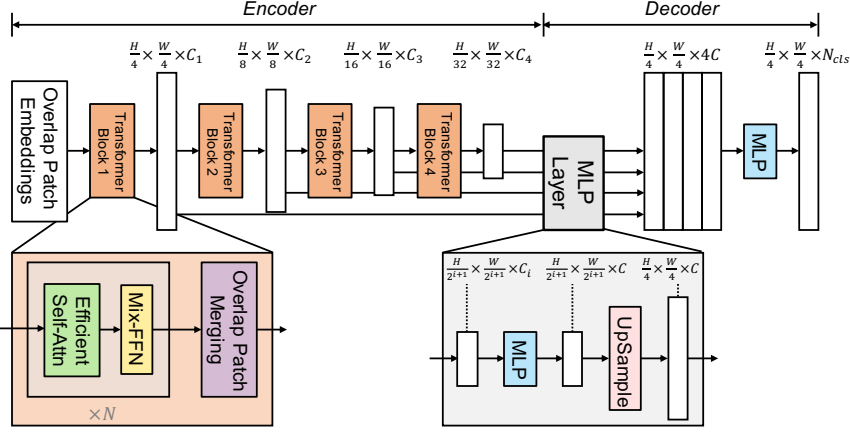


Figure 2: **The proposed SegFormer framework** consists of two main modules: A hierarchical Transformer encoder to extract coarse and fine features; and a lightweight All-MLP decoder to directly fuse these multi-level features and predict the semantic segmentation mask. “FFN” indicates feed-forward network.

2 Related Work

Semantic Segmentation. Semantic segmentation can be seen as an extension of image classification from image level to pixel level. In the deep learning era [12–14], FCN [1] is the fundamental work of semantic segmentation, which is a fully convolution network that performs pixel-to-pixel classification in an end-to-end manner. After that, researchers focused on improving FCN from different aspects such as: enlarging the receptive field [15–17, 5, 2, 4, 18]; refining the contextual information [19–27]; introducing boundary information [28–35]; designing various attention modules [36–44]; or using AutoML technologies [45–49]. These methods significantly improve semantic segmentation performance at the expense of introducing many empirical modules, making the resulting framework computationally demanding and complicated. More recent methods have proved the effectiveness of Transformer-based architectures for semantic segmentation [7, 44]. However, these methods are still computationally demanding.

Transformer backbones. ViT [6] is the first work to prove that a pure Transformer can achieve state-of-the-art performance in image classification. ViT treats each image as a sequence of tokens and then feeds them to multiple Transformer layers to make the classification. Subsequently, DeiT [50] further explores a data-efficient training strategy and a distillation approach for ViT. More recent methods such as T2T ViT [51], CPVT [52], TNT [53], CrossViT [54] and LocalViT [55] introduce tailored changes to ViT to further improve image classification performance.

Beyond classification, PVT [8] is the first work to introduce a pyramid structure in Transformer, demonstrating the potential of a pure Transformer backbone compared to CNN counterparts in dense prediction tasks. After that, methods such as Swin [9], CvT [56], CoaT [57], LeViT [58] and Twins [10] enhance the local continuity of features and remove fixed size position embedding to improve the performance of Transformers in dense prediction tasks.

Transformers for specific tasks. DETR [50] is the first to use Transformers for end-to-end object detection framework without non-maximum suppression (NMS). Other works have also used Transformers in tasks such as tracking [59, 60], super-resolution [61], re-id [62], colorization [63], retrieval [64] and multi-modal learning [65, 66]. For semantic segmentation, SETR [7] adopts ViT [6] as a backbone to extract features, achieving impressive performance. However, these Transformer-based methods have very low efficiency and, thus, difficult to deploy in real-time applications.

3 Method

As depicted in Figure 2, SegFormer consists of two main modules: (1) a hierarchical Transformer encoder; and (2) a lightweight All-MLP decoder to predict the final mask. Given an image with size $H \times W \times 3$, we first divide it into patches of size 4×4 . Unlike ViT which uses 16×16 , using fine-grained patches favors semantic segmentation. Second, we use these patches as input to the hierarchical Transformer encoder to get multi-level features with resolution $\{1/4, 1/8, 1/16, 1/32\}$

of the original image. We then pass these multi-level features to the All-MLP decoder to predict the segmentation mask with a $\frac{H}{4} \times \frac{W}{4} \times N_{cls}$ resolution, where N_{cls} is the number of categories. In the remainder of this section, we first detail the proposed encoder and decoder designs and then summarize the main differences of our approach compared to SETR.

3.1 Hierarchical Transformer Encoder

We design a series of Mix Transformer encoders (MiT), MiT-B0 to MiT-B5, with the same architecture but different sizes. On top of the hierarchical architecture and efficient self-attention module in PVT [8], we further propose several novel features including **overlapped patch merging** and **positional-encoding-free design** which will be shown to greatly benefit the segmentation tasks.

Hierarchical Feature Representation. Unlike ViT [6], our encoder generates multi-level multi-scale features given an input image. These features provide both high-resolution coarse features and low-resolution fine-grained features that boost the performance of semantic segmentation. Specifically, given an input image with size $H \times W \times 3$, we perform patch merging to obtain a hierarchical feature map F_i with a resolution of $\frac{H}{2^{i+1}} \times \frac{W}{2^{i+1}} \times C_i$, where $i \in \{1, 2, 3, 4\}$, and C_{i+1} is larger than C_i .

Efficient Self-Attention. A major bottleneck of the above hierarchical feature representation is the quadratic self-attention complexity with long sequence inputs from higher resolution features. Recall that in the original multi-head self-attention, each of the heads Q, K, V have the same dimensions $N \times C$, where $N = H \times W$ is the length of the sequence, the self-attention is estimated as:

$$\text{Attention}(Q, K, V) = \text{Softmax}\left(\frac{QK^T}{\sqrt{d_{head}}}\right)V. \quad (1)$$

We instead adopt the sequence reduction process introduced in [8]. This process uses a reduction ratio R to reduce the length of the sequence of as follows:

$$\begin{aligned} \hat{K} &= \text{Reshape}\left(\frac{N}{R}, C \cdot R\right)(K) \\ K &= \text{Linear}(C \cdot R, C)(\hat{K}), \end{aligned} \quad (2)$$

where K is the sequence to be reduced, $\text{Reshape}\left(\frac{N}{R}, C \cdot R\right)(K)$ refers to reshape K to the one with shape of $\frac{N}{R} \times (C \cdot R)$, and $\text{Linear}(C_{in}, C_{out})(\cdot)$ refers to a linear layer taking a C_{in} -dimensional tensor as input and generating a C_{out} -dimensional tensor as output. Therefore, the new K has dimensions $\frac{N}{R} \times C$. As a result, the complexity of the self-attention mechanism is reduced from $O(N^2)$ to $O\left(\frac{N^2}{R}\right)$. In our experiments, we set R to [64, 16, 4, 1] from stage-1 to stage-4.

Overlapped Patch Merging. Given an image patch, the patch merging process used in ViT, unifies a $N \times N \times 3$ patch into a $1 \times 1 \times C$ vector. This can easily be extended to unify a $2 \times 2 \times C_i$ feature path into a $1 \times 1 \times C_{i+1}$ vector to obtain hierarchical feature maps. Using this, we can shrink our hierarchical features from F_1 ($\frac{H}{4} \times \frac{W}{4} \times C_1$) to F_2 ($\frac{H}{8} \times \frac{W}{8} \times C_2$), and then iterate for any other feature map in the hierarchy. This process was initially designed to combine non-overlapping image or feature patches. Therefore, it fails to preserve the local continuity around those patches. Instead, we use an overlapping patch merging process. To this end, we define K, S , and P , where K is the patch size, S is the stride between two adjacent patches, and P is the padding size. In our experiments, we set $K = 7, S = 4, P = 3$, and $K = 3, S = 2, P = 1$ to perform overlapping patch merging to produce features with the same size as the non-overlapping process. Similar to the original patch embedding in ViT [6], this operation can be implemented by “nn.Conv2D” in PyTorch.

Positional-Encoding-Free Design. The resolution of the PE in ViT is fixed. One thus needs to interpolate the PE when the test resolution differs from training. This leads to the drop of accuracy, which is undesirable since the resolution mismatch is common in semantic segmentation. We instead introduce Mix-FFN where we consider the effect of zero padding to the leak location information [67] by directly using a 3×3 Conv in the feed-forward network (FFN). Mix-FFN is formulated as:

$$\mathbf{x}_{out} = \text{MLP}(\text{GELU}(\text{Conv}_{3 \times 3}(\text{MLP}(\mathbf{x}_{in})))) + \mathbf{x}_{in}, \quad (3)$$

where \mathbf{x}_{in} is the feature from the self-attention module. Mix-FFN mixes a 3×3 convolution and an MLP into each FFN. In our experiments, we will show that a 3×3 convolution is sufficient to provide positional information for Transformers. In particular, we use depth-wise convolutions for reducing the number of parameters and improving efficiency.

It should be mentioned that CPVT [52] also alleviates this issue by using a 3×3 Conv to generate conditional PE at different resolutions and then add it to the feature map. Our work conceptually goes one step further as we argue that adding PE to feature map is not necessary in semantic segmentation. Another recent work CvT [56] introduced 3×3 Convs to model the spatial relationship among tokens. Despite the converging design, our work differs in both motivation and application as we aim to totally remove PEs to handle the training/testing resolution mismatch issue in semantic segmentation. Our intuition started from [67] whereas the same intuition was not discussed in CvT.

3.2 Lightweight All-MLP Decoder

SegFormer incorporates a lightweight decoder consisting only of MLP layers and this avoiding the hand-crafted and computationally demanding components typically used in other methods. The key to enabling such a simple decoder is that our hierarchical Transformer encoder has a larger effective receptive field (ERF) than traditional CNN encoders.

The proposed All-MLP decoder consists of four main steps. First, multi-level features F_i from the MiT encoder go through an MLP layer to unify the channel dimension. Then, in a second step, features are up-sampled to 1/4th and concatenated together. Third, a MLP layer is adopted to fuse the concatenated features F . Finally, another MLP layer takes the fused feature to predict the segmentation mask M with a $\frac{H}{4} \times \frac{W}{4} \times N_{cls}$ resolution, where N_{cls} is the number of categories. This lets us formulate the decoder as:

$$\begin{aligned} \hat{F}_i &= \text{Linear}(C_i, C)(F_i), \forall i \\ \hat{F}_i &= \text{Upsample}\left(\frac{W}{4} \times \frac{W}{4}\right)(\hat{F}_i), \forall i \\ F &= \text{Linear}(4C, C)(\text{Concat}(\hat{F}_i)), \forall i \\ M &= \text{Linear}(C, N_{cls})(F), \end{aligned} \tag{4}$$

where M refers to the predicted mask, and $\text{Linear}(C_{in}, C_{out})(\cdot)$ refers to a linear layer with C_{in} and C_{out} as input and output vector dimensions respectively.

Effective Receptive Field Analysis.

For semantic segmentation, maintaining large receptive field to include context information has been a central issue [5, 17, 18]. Here, we use effective receptive field (ERF) [68] as a toolkit to visualize and interpret why our MLP decoder design is so effective on Transformers. In Figure 3, we visualize ERFs of the four encoder stages and the decoder heads for both DeepLabv3+ and SegFormer. We can make the following observations:

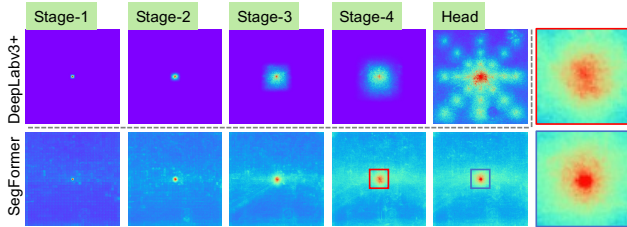


Figure 3: **Effective Receptive Field (ERF) on Cityscapes** (average over 100 images). Top row: DeepLabv3+. Bottom row: SegFormer. ERFs of the four stages and the decoder heads of both architectures are visualized. Best viewed with zoom in.

- The ERF of DeepLabv3+ is relatively small even at Stage-4, the deepest stage.
- SegFormer’s encoder naturally produces local attentions which resemble convolutions at lower stages, while able to output highly non-local attentions that effectively capture contexts at Stage-4.
- As shown with the zoom-in patches in Figure 3, the ERF of the MLP head (blue box) differs from Stage-4 (red box) with a significant stronger local attention besides the non-local attention.

The limited receptive field in CNN requires one to resort to context modules such as ASPP [16] that enlarge the receptive field but inevitably become heavy. Our decoder design benefits from the non-local attention in Transformers and leads to a larger receptive field without being complex. The same decoder design, however, does not work well on CNN backbones since the overall receptive field is upper bounded by the limited one at Stage-4, and we will verify this later in Table 1d,

More importantly, our decoder design essentially takes advantage of a Transformer induced feature that produces both highly local and non-local attention at the same time. By unifying them, our MLP decoder renders complementary and powerful representations by adding few parameters. This is

another key reason that motivated our design. Taking the non-local attention from Stage-4 alone is not enough to produce good results, as will be verified in Table 1d.

3.3 Relationship to SETR.

SegFormer contains multiple more efficient and powerful designs compared with SETR [7]:

- We only use ImageNet-1K for pre-training. ViT in SETR is pre-trained on larger ImageNet-22K.
- SegFormer’s encoder has a hierarchical architecture, which is smaller than ViT and can capture both high-resolution coarse and low-resolution fine features. In contrast, SETR’s ViT encoder can only generate single low-resolution feature map.
- We remove Positional Embedding in encoder, while SETR uses fixed shape Positional Embedding which decreases the accuracy when the resolution at inference differs from the training ones.
- Our MLP decoder is more compact and less computationally demanding than the one in SETR. This leads to a *negligible* computational overhead. In contrast, SETR requires heavy decoders with multiple 3×3 convolutions.

4 Experiments

4.1 Experimental Settings

Datasets: We used four public datasets: Cityscapes [69], ADE20K [70], and COCO-Stuff [71]. ADE20K is a dataset covering 150 fine-grained semantic concepts consisting of 20210 images. Cityscapes is a driving dataset for semantic segmentation consisting of 5000 fine-annotated high resolution images with 19 categories. COCO-Stuff covers 172 labels and consists of 164k images: 118k for training, 5k for validation, 20k for test-dev and 20k for the test-challenge.

Implementation details: We used the *mmsegmentation*² codebase and train on a server with 8 Tesla V100. We pre-train the encoder on the Imagenet-1K dataset and randomly initialize the decoder. During training, we applied data augmentation through random resize with ratio 0.5-2.0, random horizontal flipping, and random cropping to 512×512 , 1024×1024 , 512×512 for ADE20K, Cityscapes and COCO-Stuff. Following [9] we set crop size to 640×640 on ADE20K for our largest model B5. We trained the models using AdamW optimizer for 160K iterations on ADE20K, Cityscapes, and 80K iterations on COCO-Stuff. Exceptionally, for the ablation studies, we trained the models for 40K iterations. We used a batch size of 16 for ADE20K, COCO-Stuff and a batch size of 8 for Cityscapes. The learning rate was set to an initial value of 0.00006 and then used a “poly” LR schedule with factor 1.0 by default. For simplicity, we *did not* adopt widely-used tricks such as OHEM, auxiliary losses or class balance loss. During evaluation, we rescale the short side of the image to training cropping size and keep the aspect ratio for ADE20K and COCO-Stuff. For Cityscapes, we do inference using sliding window test by cropping 1024×1024 windows. We report semantic segmentation performance using mean Intersection over Union (mIoU).

4.2 Ablation Studies

Influence of the size of model. We first analyze the effect of increasing the size of the encoder on the performance and model efficiency. Figure 1 shows the performance vs. model efficiency for ADE20K as a function of the encoder size and, Table 1a summarizes the results for the three datasets. The first thing to observe here is the size of the decoder compared to the encoder. As shown, for the lightweight model, the decoder has only 0.4M parameters. For MiT-B5 encoder, the decoder only takes up to 4% of the total number of parameters in the model. In terms of performance, we can observe that, overall, increasing the size of the encoder yields consistent improvements on all the datasets. Our lightweight model, SegFormer-B0, is compact and efficient while maintaining a competitive performance, showing that our method is very convenient for real-time applications. On the other hand, our SegFormer-B5, the largest model, achieves state-of-the-art results on all three datasets, showing the potential of our Transformer encoder.

²<https://github.com/open-mmlab/msegmentation>

Table 1: Ablation studies related to model size, encoder and decoder design.

(a) Accuracy, parameters and flops as a function of the model size on the three datasets. ‘‘SS’’ and ‘‘MS’’ means single/multi-scale test.

Encoder Model Size	Params		ADE20K		Cityscapes		COCO-Stuff	
	Encoder	Decoder	Flops ↓	mIoU(SS/MS) ↑	Flops ↓	mIoU(SS/MS) ↑	Flops ↓	mIoU(SS) ↑
MiT-B0	3.4	0.4	8.4	37.4 / 38.0	125.5	76.2 / 78.1	8.4	35.6
MiT-B1	13.1	0.6	15.9	42.2 / 43.1	243.7	78.5 / 80.0	15.9	40.2
MiT-B2	24.2	3.3	62.4	46.5 / 47.5	717.1	81.0 / 82.2	62.4	44.6
MiT-B3	44.0	3.3	79.0	49.4 / 50.0	962.9	81.7 / 83.3	79.0	45.5
MiT-B4	60.8	3.3	95.7	50.3 / 51.1	1240.6	82.3 / 83.9	95.7	46.5
MiT-B5	81.4	3.3	183.3	51.0 / 51.8	1460.4	82.4 / 84.0	111.6	46.7

(b) Accuracy as a function of the MLP dimension C in the decoder on ADE20K.

C	Flops ↓	Params ↓	mIoU ↑
256	25.7	24.7	44.9
512	39.8	25.8	45.0
768	62.4	27.5	45.4
1024	93.6	29.6	45.2
2048	304.4	43.4	45.6

(c) Mix-FFN vs. positional encoding (PE) for different test resolution on Cityscapes.

Inf Res	Enc Type	mIoU ↑
768×768	PE	77.3
1024×2048	PE	74.0
768×768	Mix-FFN	80.5
1024×2048	Mix-FFN	79.8

(d) Accuracy on ADE20K of CNN and Transformer encoder with MLP decoder. ‘‘S4’’ means stage-4 feature.

Encoder	Flops ↓	Params ↓	mIoU ↑
ResNet50 (S1-4)	69.2	29.0	34.7
ResNet101 (S1-4)	88.7	47.9	38.7
ResNeXt101 (S1-4)	127.5	86.8	39.8
MiT-B2 (S4)	22.3	24.7	43.1
MiT-B2 (S1-4)	62.4	27.7	45.4
MiT-B3 (S1-4)	79.0	47.3	48.6

Table 2: Comparison to state of the art methods on ADE20K and Cityscapes. SegFormer has significant advantages on #Params (M), #Flops, #Speed and #Accuracy. Note that for SegFormer-B0 we scale the short side of image to {1024, 768, 640, 512} to get speed-accuracy tradeoffs.

	Method	Encoder	Params ↓	ADE20K			Cityscapes		
				Flops ↓	FPS ↑	mIoU ↑	Flops ↓	FPS ↑	mIoU ↑
Real-Time	FCN [1]	MobileNetV2	9.8	39.6	64.4	19.7	317.1	14.2	61.5
	ICNet [11]	-	-	-	-	-	-	30.3	67.7
	PSPNet [15]	MobileNetV2	13.7	52.9	57.7	29.6	423.4	11.2	70.2
	DeepLabV3+ [18]	MobileNetV2	15.4	69.4	43.1	34.0	555.4	8.4	75.2
Real-Time	SegFormer (Ours)	MiT-B0	3.8	8.4	50.5	37.4	125.5	15.2	76.2
				-	-	-	51.7	26.3	75.3
				-	-	-	31.5	37.1	73.7
				-	-	-	17.7	47.6	71.9
Non Real-Time	FCN [1]	ResNet-101	68.6	275.7	14.8	41.4	2203.3	1.2	76.6
	EncNet [22]	ResNet-101	55.1	218.8	14.9	44.7	1748.0	1.3	76.9
	PSPNet [15]	ResNet-101	68.1	256.4	15.3	44.4	2048.9	1.2	78.5
	CCNet [39]	ResNet-101	68.9	278.4	14.1	45.2	2224.8	1.0	80.2
	DeeplabV3+ [18]	ResNet-101	62.7	255.1	14.1	44.1	2032.3	1.2	80.9
	OCRNet [21]	HRNet-W48	70.5	164.8	17.0	45.6	1296.8	4.2	81.1
	GSCNN [33]	WideResNet38	-	-	-	-	-	-	80.8
	Axial-DeepLab [72]	AxialResNet-XL	-	-	-	-	2446.8	-	81.1
	Dynamic Routing [73]	Dynamic-L33-PSP	-	-	-	-	270.0	-	80.7
	Auto-Deeplab [48]	NAS-F48-ASPP	-	-	-	44.0	695.0	-	80.3
	SETR [7]	ViT-Large	318.3	-	5.4	50.2	-	0.5	82.2
	SegFormer (Ours)	MiT-B4	64.1	95.7	15.4	51.1	1240.6	3.0	83.8
	SegFormer (Ours)	MiT-B5	84.7	183.3	9.8	51.8	1447.6	2.5	84.0

Influence of C , the MLP decoder channel dimension. We now analyze the influence of the channel dimension C in the MLP decoder, see Section 3.2. In Table 1b we show performance, flops, and parameters as a function of this dimension. We can observe that setting $C = 256$ provides a very competitive performance and computational cost. The performance increases as C increases; however, it leads to larger and less efficient models. Interestingly, this performance plateaus for channel dimensions wider than 768. Given these results, we choose $C = 256$ for our real-time models SegFormer-B0, B1 and $C = 768$ for the rest.

Mix-FFN vs. Positional Encoder (PE). In this experiment, we analyze the effect of removing the positional encoding in the Transformer encoder in favor of using the proposed Mix-FFN. To this end, we train Transformer encoders with a positional encoding (PE) and the proposed Mix-FFN and perform inference on Cityscapes with two different image resolutions: 768×768 using a sliding window, and 1024×2048 using the whole image.

Table 1c shows the results for this experiment. As shown, for a given resolution, our approach using Mix-FFN clearly outperforms using a positional encoding. Moreover, our approach is less sensitive to differences in the test resolution: the accuracy drops 3.3% when using a positional encoding with a

lower resolution. In contrast, when we use the proposed Mix-FFN the performance drop is reduced to only 0.7%. From these results, we can conclude using the proposed Mix-FFN produces better and more robust encoders than those using positional encoding.

Effective receptive field evaluation. In Section 3.2, we argued that our MLP decoder benefits from Transformers having a larger effective receptive field compared to other CNN models. To quantify this effect, in this experiment, we compare the performance of our MLP-decoder when used with CNN-based encoders such as ResNet or ResNeXt. As shown in Table 1d, coupling our MLP-decoder with a CNN-based encoder yields a significantly lower accuracy compared to coupling it with the proposed Transformer encoder. Intuitively, as a CNN has a smaller receptive field than the Transformer (see the analysis in Section 3.2), the MLP-decoder is not enough for global reasoning. In contrast, coupling our Transformer encoder with the MLP decoder leads to the best performance. Moreover, for Transformer encoder, it is necessary to combine low-level local features and high-level non-local features instead of only high-level feature.

Influence of difference encoders. We select 2 representative Transformer encoders, ViT [6] and Swin [9] and compare with our MiT encoder. As shown in Table 3, with same decoder, e.g. MLP decoder, MiT-B2 is 3.1% higher than Swin-T with similar encoder parameters. Moreover, MiT-B5 has much fewer encoder parameters than ViT-large, but is 3+% mIoU higher than ViT-large. These experiments shows our MiT encoder is better than Swin and ViT for semantic segmentation.

Influence of difference decoders. We also test MiT encoder with different decoders. As shown in Table 3, the mIoUs are similar with different decoders while the proposed MLP decoder has the least parameters and is only 1/8 of the UperNet decoder in Swin. The MLP decoder is thus an important design towards efficient segmentation.

Table 3: Ablation study of different Transformer encoders and different decoders. All the model are trained on ADE20K with 160K iterations.

Encoder	Decoder	mIoU	FPS	Decoder GFlops	Decoder Params (M)
MiT-B2	UperNet (Swin)	46.5	14.2	210.7	29.7
MiT-B2	MLA (SETR)	46.2	9.5	87.7	4.2
MiT-B2	MLP (Ours)	46.5	21.4	42.1	3.3
MiT-B5	UperNet (Swin)	50.7	5.3	210.7	29.7
MiT-B5	MLA (SETR)	50.9	3.8	87.7	4.2
MiT-B5	MLP (Ours)	51.0	9.8	42.1	3.3
Swin-T	MLP (Ours)	43.4	20.6	42.8	3.6
Swin-T	UperNet (Swin)	44.5	15.4	211.3	31.4
ViT-L	MLP (Ours)	47.7	4.7	0.6	0.6
ViT-L	MLA (SETR)	47.7	4.6	1.8	3.7

4.3 Comparison to state of the art methods

We now compare our results with existing approaches on the ADE20K [70] and Cityscapes [69]. More experiments about COCO-Stuff [71] are in appendix.

ADE20K and Cityscapes: Table 2 summarizes our results including parameters, FLOPS, latency, and accuracy for ADE20K and Cityscapes. In the top part of the table, we report real-time approaches where we include state-of-the-art methods and our results using the MiT-B0 lightweight encoder. In the bottom part, we focus on performance and report the results of our approach and related works using stronger encoders.

On ADE20K, SegFormer-B0 yields 37.4% mIoU using only 3.8M parameters and 8.4G FLOPs, outperforming all other real-time counterparts in terms of parameters, flops, and latency. For instance, compared to DeeplabV3+ (MobileNetV2), SegFormer-B0 is 7.4 FPS, which is faster and keeps 3.4% better mIoU.

Moreover, SegFormer-B5 outperforms all other approaches, including the previous best SETR, and establishes a new state-of-the-art of 51.8%, which is 1.6% mIoU better than SETR while being significantly more efficient.

Table 4: Comparison to state of the art methods on Cityscapes test set. IM-1K, IM-22K, Coarse and MV refer to the ImageNet-1K, ImageNet-22K, Cityscapes coarse set and Mapillary Vistas.

Method	Encoder	Extra Data	mIoU
PSPNet [15]	ResNet-101	IM-1K	78.4
PSANet [41]	ResNet-101	IM-1K	80.1
CCNet [39]	ResNet-101	IM-1K	81.9
OCNet [19]	ResNet-101	IM-1K	80.1
Axial-DeepLab [72]	AxialResNet-XL	IM-1K	79.9
SETR [7]	ViT	IM-22K	81.0
SETR [7]	ViT	IM-22K, Coarse	81.6
SegFormer	MiT-B5	IM-1K	82.2
SegFormer	MiT-B5	IM-1K, MV	83.1

As also shown in Table 2, our results also hold on Cityscapes. SegFormer-B0 yields 15.2 FPS and 76.2% mIoU (the shorter side of input image being 1024), which represents a 1.3% mIoU improvement and a 2× speedup compared to DeeplabV3+. Moreover, with the shorter side of input image being 512, SegFormer-B0 runs at 47.6 FPS and yields 71.9% mIoU, which is 17.3 FPS faster and 4.2% better than ICNet. SegFormer-B5 archives the best IoU of 84.0%, outperforming all existing

methods by at least 1.8% mIoU, and it runs $5 \times$ faster and $4 \times$ smaller than SETR [7]. On Cityscapes test set, we follow the common setting [18] and merge the validation images to the train set and report results using Imagenet-1K pre-training and also using Mapillary Vistas [74]. As reported in Table 4, using only Cityscapes fine data and Imagenet-1K pre-training, our method achieves 82.2% mIoU outperforming all other methods including SETR, which uses ImageNet-22K pre-training and the additional Cityscapes coarse data. Using Mapillary pre-training, our sets a new state-of-the-art result of 83.1% mIoU.

4.4 Robustness to natural corruptions

Model robustness is important for many safety-critical tasks such as autonomous driving [75]. In this experiment, we evaluate the robustness of SegFormer to common corruptions and perturbations. To this end, we follow [75] and generate Cityscapes-C, which expands the Cityscapes validation set with 16 types of algorithmically generated corruptions from noise, blur, weather and digital categories. We compare our method to DeeplabV3+ and other methods as reported in [75]. We also compare with SETR with DeiT Transformer backbone. The results for this experiment are summarized in Table 5.

Our method significantly outperforms previous CNN-based methods, yielding a relative improvement of up to 588% on Gaussian Noise and up to 295% on snow weather. SegFormer also outperforms SETR in general except for one corruption (snow). The results indicate the strong robustness of SegFormer, which we envision to benefit safety-critical applications where robustness is important.

Table 5: **Main results on Cityscapes-C**. “DLv3+”, “MBv2”, “R” and “X” refer to DeepLabv3+, MobileNetv2, ResNet and Xception. The mIoUs of compared methods are reported from [75].

Method	Clean	Blur				Noise				Digital				Weather			
		Motion	Defoc	Glass	Gauss	Gauss	Impul	Shot	Speck	Bright	Contr	Satur	JPEG	Snow	Spatt	Fog	Frost
DLv3+ (MBv2)	72.0	53.5	49.0	45.3	49.1	6.4	7.0	6.6	16.6	51.7	46.7	32.4	27.2	13.7	38.9	47.4	17.3
DLv3+ (R50)	76.6	58.5	56.6	47.2	57.7	6.5	7.2	10.0	31.1	58.2	54.7	41.3	27.4	12.0	42.0	55.9	22.8
DLv3+ (R101)	77.1	59.1	56.3	47.7	57.3	13.2	13.9	16.3	36.9	59.2	54.5	41.5	37.4	11.9	47.8	55.1	22.7
DLv3+ (X41)	77.8	61.6	54.9	51.0	54.7	17.0	17.3	21.6	43.7	63.6	56.9	51.7	38.5	18.2	46.6	57.6	20.6
DLv3+ (X65)	78.4	63.9	59.1	52.8	59.2	15.0	10.6	19.8	42.4	65.9	59.1	46.1	31.4	19.3	50.7	63.6	23.8
DLv3+ (X71)	78.6	64.1	60.9	52.0	60.4	14.9	10.8	19.4	41.2	68.0	58.7	47.1	40.2	18.8	50.4	64.1	20.2
ICNet	65.9	45.8	44.6	47.4	44.7	8.4	8.4	10.6	27.9	41.0	33.1	27.5	34.0	6.3	30.5	27.3	11.0
FCN8s	66.7	42.7	31.1	37.0	34.1	6.7	5.7	7.8	24.9	53.3	39.0	36.0	21.2	11.3	31.6	37.6	19.7
DilatedNet	68.6	44.4	36.3	32.5	38.4	15.6	14.0	18.4	32.7	52.7	32.6	38.1	29.1	12.5	32.3	34.7	19.2
ResNet-38	77.5	54.6	45.1	43.3	47.2	13.7	16.0	18.2	38.3	60.0	50.6	46.9	14.7	13.5	45.9	52.9	22.2
PSPNet	78.8	59.8	53.2	44.4	53.9	11.0	15.4	15.4	34.2	60.4	51.8	30.6	21.4	8.4	42.7	34.4	16.2
GSCNN	80.9	58.9	58.4	41.9	60.1	5.5	2.6	6.8	24.7	75.9	61.9	70.7	12.0	12.4	47.3	67.9	32.6
SETR-DeiT	78.9	64.9	65.1	59.1	65.3	54.7	60.5	51.9	69.4	74.9	69.6	74.9	58.5	44.3	64.8	68.2	39.1
SegFormer-B5	82.4	69.1	68.6	64.1	69.8	57.8	63.4	52.3	72.8	81.0	77.7	80.1	58.8	40.7	68.4	78.5	49.9

5 Conclusion

In this paper, we present SegFormer, a simple, clean yet powerful semantic segmentation method which contains a positional-encoding-free, hierarchical Transformer encoder and a lightweight All-MLP decoder. It avoids common complex designs in previous methods, leading to both high efficiency and performance. SegFormer not only achieves new state of the art results on common datasets, but also shows strong zero-shot robustness. We hope our method can serve as a solid baseline for semantic segmentation and motivate further research. One potential limitation is that even our lightest model may still be too heavy for some edge devices. Thus mixed-precision training, pruning, hardware-friendly attention designs and energy consumption are important parts of our future work.

Broader Impact

Efficiency, accuracy, and robustness are important aspects of AI models. Our work pushes the boundary of semantic segmentation models in these three aspects. We envision that the work will benefit a wide range of safety-critical applications, such as autonomous driving and robot navigation. The proposed method improves the “in-the-wild” robustness of these applications, ultimately leading to better safety. Despite such improvement, we fully understand this work is by no means perfect and there are still many challenges towards reliable real world application. Our models may be subject to biases and other possible undesired mistakes, depending on how they are trained in reality. Our

model may also be used for surveillance similar to other AI recognition methods, even though it is not mainly designed for surveillance applications.

Acknowledgments and Disclosure of Funding

We thank Ding Liang, Zhe Chen and Yaojun Liu for insightful discussion without which this paper would not be possible. Ping Luo is supported by the General Research Fund of Hong Kong No.27208720.

References

- [1] Jonathan Long, Evan Shelhamer, and Trevor Darrell. Fully convolutional networks for semantic segmentation. In *CVPR*, 2015. 1, 2, 3, 7
- [2] Liang-Chieh Chen, George Papandreou, Iasonas Kokkinos, Kevin Murphy, and Alan L Yuille. Semantic image segmentation with deep convolutional nets and fully connected CRFs. In *ICLR*, 2015. 2, 3
- [3] Hang Zhang, Chongruo Wu, Zhongyue Zhang, Yi Zhu, Haibin Lin, Zhi Zhang, Yue Sun, Tong He, Jonas Mueller, R Manmatha, et al. ResNest: Split-attention networks. *arXiv*, 2020. 2
- [4] Liang-Chieh Chen, George Papandreou, Iasonas Kokkinos, Kevin Murphy, and Alan L Yuille. Deeplab: Semantic image segmentation with deep convolutional nets, atrous convolution, and fully connected CRFs. *TPAMI*, 2017. 2, 3
- [5] Fisher Yu and Vladlen Koltun. Multi-scale context aggregation by dilated convolutions. In *ICLR*, 2016. 2, 3, 5
- [6] Alexey Dosovitskiy, Lucas Beyer, Alexander Kolesnikov, Dirk Weissenborn, Xiaohua Zhai, Thomas Unterthiner, Mostafa Dehghani, Matthias Minderer, Georg Heigold, Sylvain Gelly, et al. An image is worth 16x16 words: Transformers for image recognition at scale. *arXiv*, 2020. 2, 3, 4, 8
- [7] Sixiao Zheng, Jiachen Lu, Hengshuang Zhao, Xiatian Zhu, Zekun Luo, Yabiao Wang, Yanwei Fu, Jianfeng Feng, Tao Xiang, Philip HS Torr, et al. Rethinking semantic segmentation from a sequence-to-sequence perspective with transformers. *CVPR*, 2021. 2, 3, 6, 7, 8, 9
- [8] Wenhai Wang, Enze Xie, Xiang Li, Deng-Ping Fan, Kaitao Song, Ding Liang, Tong Lu, Ping Luo, and Ling Shao. Pyramid vision transformer: A versatile backbone for dense prediction without convolutions. *arXiv*, 2021. 2, 3, 4
- [9] Ze Liu, Yutong Lin, Yue Cao, Han Hu, Yixuan Wei, Zheng Zhang, Stephen Lin, and Baining Guo. Swin transformer: Hierarchical vision transformer using shifted windows. *arXiv*, 2021. 2, 3, 6, 8
- [10] Xiangxiang Chu, Zhi Tian, Yuqing Wang, Bo Zhang, Haibing Ren, Xiaolin Wei, Huaxia Xia, and Chunhua Shen. Twins: Revisiting spatial attention design in vision transformers. *arXiv*, 2021. 2, 3
- [11] Hengshuang Zhao, Xiaojuan Qi, Xiaoyong Shen, Jianping Shi, and Jiaya Jia. Icnet for real-time semantic segmentation on high-resolution images. In *ECCV*, 2018. 2, 7
- [12] Kaiming He, Xiangyu Zhang, Shaoqing Ren, and Jian Sun. Deep residual learning for image recognition. In *CVPR*, 2016. 3
- [13] Alex Krizhevsky, Ilya Sutskever, and Geoffrey E Hinton. Imagenet classification with deep convolutional neural networks. *NeurIPS*, 2012.
- [14] Karen Simonyan and Andrew Zisserman. Very deep convolutional networks for large-scale image recognition. *arXiv*, 2014. 3
- [15] Hengshuang Zhao, Jianping Shi, Xiaojuan Qi, Xiaogang Wang, and Jiaya Jia. Pyramid scene parsing network. In *CVPR*, 2017. 3, 7, 8
- [16] Maoke Yang, Kun Yu, Chi Zhang, Zhiwei Li, and Kuiyuan Yang. Denseaspp for semantic segmentation in street scenes. In *CVPR*, 2018. 5
- [17] Chao Peng, Xiangyu Zhang, Gang Yu, Guiming Luo, and Jian Sun. Large kernel matters—improve semantic segmentation by global convolutional network. In *CVPR*, 2017. 3, 5

- [18] Liang-Chieh Chen, Yukun Zhu, George Papandreou, Florian Schroff, and Hartwig Adam. Encoder-decoder with atrous separable convolution for semantic image segmentation. In *ECCV*, 2018. 3, 5, 7, 9
- [19] Yuhui Yuan and Jingdong Wang. Ocnet: Object context network for scene parsing. *arXiv*, 2018. 3, 8
- [20] Changqian Yu, Jingbo Wang, Changxin Gao, Gang Yu, Chunhua Shen, and Nong Sang. Context prior for scene segmentation. In *CVPR*, 2020.
- [21] Yuhui Yuan, Xilin Chen, and Jingdong Wang. Object-contextual representations for semantic segmentation. *arXiv*, 2019. 7
- [22] Hang Zhang, Kristin Dana, Jianping Shi, Zhongyue Zhang, Xiaogang Wang, Amrith Tyagi, and Amit Agrawal. Context encoding for semantic segmentation. In *CVPR*, 2018. 7
- [23] Yizhou Zhou, Xiaoyan Sun, Zheng-Jun Zha, and Wenjun Zeng. Context-reinforced semantic segmentation. In *CVPR*, 2019.
- [24] Guosheng Lin, Anton Milan, Chunhua Shen, and Ian Reid. Refinenet: Multi-path refinement networks for high-resolution semantic segmentation. In *CVPR*, 2017.
- [25] Rudra PK Poudel, Ujwal Bonde, Stephan Liwicki, and Christopher Zach. Contextnet: Exploring context and detail for semantic segmentation in real-time. *arXiv*, 2018.
- [26] Tianyi Wu, Sheng Tang, Rui Zhang, and Yongdong Zhang. Cgnet: A light-weight context guided network for semantic segmentation. *arXiv*, 2018.
- [27] Junjun He, Zhongying Deng, Lei Zhou, Yali Wang, and Yu Qiao. Adaptive pyramid context network for semantic segmentation. In *CVPR*, 2019. 3
- [28] Henghui Ding, Xudong Jiang, Ai Qun Liu, Nadia Magnenat Thalmann, and Gang Wang. Boundary-aware feature propagation for scene segmentation. In *ICCV*, 2019. 3
- [29] Gedas Bertasius, Jianbo Shi, and Lorenzo Torresani. Semantic segmentation with boundary neural fields. In *CVPR*, 2016.
- [30] Xiangtai Li, Xia Li, Li Zhang, Guangliang Cheng, Jianping Shi, Zhouchen Lin, Shaohua Tan, and Yunhai Tong. Improving semantic segmentation via decoupled body and edge supervision. *arxiv*, 2020.
- [31] Yuhui Yuan, Jingyi Xie, Xilin Chen, and Jingdong Wang. Segfix: Model-agnostic boundary refinement for segmentation. In *ECCV*, 2020.
- [32] Mingmin Zhen, Jinglu Wang, Lei Zhou, Shiwei Li, Tianwei Shen, Jiayang Shang, Tian Fang, and Long Quan. Joint semantic segmentation and boundary detection using iterative pyramid contexts. In *CVPR*, 2020.
- [33] Towaki Takikawa, David Acuna, Varun Jampani, and Sanja Fidler. Gated-scnn: Gated shape cnns for semantic segmentation. In *ICCV*, 2019. 7
- [34] Changqian Yu, Jingbo Wang, Chao Peng, Changxin Gao, Gang Yu, and Nong Sang. Learning a discriminative feature network for semantic segmentation. In *CVPR*, 2018.
- [35] Liang-Chieh Chen, Jonathan T Barron, George Papandreou, Kevin Murphy, and Alan L Yuille. Semantic image segmentation with task-specific edge detection using cnns and a discriminatively trained domain transform. In *CVPR*, 2016. 3
- [36] Jun Fu, Jing Liu, Haijie Tian, Yong Li, Yongjun Bao, Zhiwei Fang, and Hanqing Lu. Dual attention network for scene segmentation. In *CVPR*, 2019. 3
- [37] Xiaolong Wang, Ross Girshick, Abhinav Gupta, and Kaiming He. Non-local neural networks. In *CVPR*, 2018.
- [38] Zilong Zhong, Zhong Qiu Lin, Rene Bidart, Xiaodan Hu, Ibrahim Ben Daya, Zhifeng Li, Wei-Shi Zheng, Jonathan Li, and Alexander Wong. Squeeze-and-attention networks for semantic segmentation. In *CVPR*, 2020.
- [39] Zilong Huang, Xinggang Wang, Lichao Huang, Chang Huang, Yunchao Wei, and Wenyu Liu. Ccnet: Criss-cross attention for semantic segmentation. In *ICCV*, 2019. 7, 8
- [40] Hanchao Li, Pengfei Xiong, Jie An, and Lingxue Wang. Pyramid attention network for semantic segmentation. *arXiv*, 2018.

- [41] Hengshuang Zhao, Yi Zhang, Shu Liu, Jianping Shi, Chen Change Loy, Dahua Lin, and Jiaya Jia. Psanet: Point-wise spatial attention network for scene parsing. In *ECCV*, 2018. 8
- [42] Xia Li, Zhisheng Zhong, Jianlong Wu, Yibo Yang, Zhouchen Lin, and Hong Liu. Expectation-maximization attention networks for semantic segmentation. In *ICCV*, 2019.
- [43] Yue Cao, Jiarui Xu, Stephen Lin, Fangyun Wei, and Han Hu. Gcnnet: Non-local networks meet squeeze-excitation networks and beyond. In *ICCVW*, 2019.
- [44] Enze Xie, Wenjia Wang, Wenhai Wang, Peize Sun, Hang Xu, Ding Liang, and Ping Luo. Segmenting transparent object in the wild with transformer. *IJCAI*, 2021. 3
- [45] Albert Shaw, Daniel Hunter, Forrest Landola, and Sammy Sidhu. Squeezenas: Fast neural architecture search for faster semantic segmentation. In *ICCVW*, 2019. 3
- [46] Wuyang Chen, Xinyu Gong, Xianming Liu, Qian Zhang, Yuan Li, and Zhangyang Wang. Fasterseg: Searching for faster real-time semantic segmentation. *arXiv*, 2019.
- [47] Yanwei Li, Lin Song, Yukang Chen, Zeming Li, Xiangyu Zhang, Xingang Wang, and Jian Sun. Learning dynamic routing for semantic segmentation. In *CVPR*, 2020.
- [48] Chenxi Liu, Liang-Chieh Chen, Florian Schroff, Hartwig Adam, Wei Hua, Alan L Yuille, and Li Fei-Fei. Auto-deeplab: Hierarchical neural architecture search for semantic image segmentation. In *CPVR*, 2019. 7
- [49] Vladimir Nekrasov, Hao Chen, Chunhua Shen, and Ian Reid. Fast neural architecture search of compact semantic segmentation models via auxiliary cells. In *CVPR*, 2019. 3
- [50] Nicolas Carion, Francisco Massa, Gabriel Synnaeve, Nicolas Usunier, Alexander Kirillov, and Sergey Zagoruyko. End-to-End object detection with transformers. In *ECCV*, 2020. 3
- [51] Li Yuan, Yunpeng Chen, Tao Wang, Weihao Yu, Yujun Shi, Zihang Jiang, Francis EH Tay, Jiashi Feng, and Shuicheng Yan. Tokens-to-token vit: Training vision transformers from scratch on imagenet. *arXiv*, 2021. 3
- [52] Xiangxiang Chu, Zhi Tian, Bo Zhang, Xinlong Wang, Xiaolin Wei, Huaxia Xia, and Chunhua Shen. Conditional positional encodings for vision transformers. *arXiv*, 2021. 3, 5
- [53] Kai Han, An Xiao, Enhua Wu, Jianyuan Guo, Chunjing Xu, and Yunhe Wang. Transformer in transformer. *arXiv*, 2021. 3
- [54] Chun-Fu Chen, Quanfu Fan, and Rameswar Panda. Crossvit: Cross-attention multi-scale vision transformer for image classification. *arXiv*, 2021. 3
- [55] Yawei Li, Kai Zhang, Jiezhong Cao, Radu Timofte, and Luc Van Gool. Localvit: Bringing locality to vision transformers. *arXiv*, 2021. 3
- [56] Haiping Wu, Bin Xiao, Noel Codella, Mengchen Liu, Xiyang Dai, Lu Yuan, and Lei Zhang. Cvt: Introducing convolutions to vision transformers. *arXiv*, 2021. 3, 5
- [57] Weijian Xu, Yifan Xu, Tyler Chang, and Zhuowen Tu. Co-scale conv-attentional image transformers. *arXiv*, 2021. 3
- [58] Ben Graham, Alaaeldin El-Nouby, Hugo Touvron, Pierre Stock, Armand Joulin, Hervé Jégou, and Matthijs Douze. Levit: a vision transformer in convnet’s clothing for faster inference. *arXiv*, 2021. 3
- [59] Peize Sun, Yi Jiang, Rufeng Zhang, Enze Xie, Jinkun Cao, Xinting Hu, Tao Kong, Zehuan Yuan, Changhu Wang, and Ping Luo. Transtrack: Multiple-object tracking with transformer. *arXiv*, 2020. 3
- [60] Tim Meinhardt, Alexander Kirillov, Laura Leal-Taixe, and Christoph Feichtenhofer. Trackformer: Multi-object tracking with transformers. *arXiv*, 2021. 3
- [61] Hanting Chen, Yunhe Wang, Tianyu Guo, Chang Xu, Yiping Deng, Zhenhua Liu, Siwei Ma, Chunjing Xu, Chao Xu, and Wen Gao. Pre-trained image processing transformer. *arXiv*, 2020. 3
- [62] Shuting He, Hao Luo, Pichao Wang, Fan Wang, Hao Li, and Wei Jiang. Transreid: Transformer-based object re-identification. *arXiv*, 2021. 3
- [63] Manoj Kumar, Dirk Weissenborn, and Nal Kalchbrenner. Colorization transformer. *arXiv*, 2021. 3

- [64] Alaaeldin El-Nouby, Natalia Neverova, Ivan Laptev, and Hervé Jégou. Training vision transformers for image retrieval. *arXiv*, 2021. [3](#)
- [65] Alec Radford, Jong Wook Kim, Chris Hallacy, Aditya Ramesh, Gabriel Goh, Sandhini Agarwal, Girish Sastry, Amanda Askell, Pamela Mishkin, Jack Clark, et al. Learning transferable visual models from natural language supervision. *arXiv*, 2021. [3](#)
- [66] Ronghang Hu and Amanpreet Singh. Transformer is all you need: Multimodal multitask learning with a unified transformer. *arXiv*, 2021. [3](#)
- [67] Md Amirul Islam, Sen Jia, and Neil DB Bruce. How much position information do convolutional neural networks encode? *arXiv*, 2020. [4](#), [5](#)
- [68] Wenjie Luo, Yujia Li, Raquel Urtasun, and Richard Zemel. Understanding the effective receptive field in deep convolutional neural networks. *arXiv*, 2017. [5](#)
- [69] Marius Cordts, Mohamed Omran, Sebastian Ramos, Timo Rehfeld, Markus Enzweiler, Rodrigo Benenson, Uwe Franke, Stefan Roth, and Bernt Schiele. The cityscapes dataset for semantic urban scene understanding. In *CVPR*, 2016. [6](#), [8](#)
- [70] Bolei Zhou, Hang Zhao, Xavier Puig, Sanja Fidler, Adela Barriuso, and Antonio Torralba. Scene parsing through ade20k dataset. In *CVPR*, 2017. [6](#), [8](#)
- [71] Holger Caesar, Jasper Uijlings, and Vittorio Ferrari. Coco-stuff: Thing and stuff classes in context. In *CVPR*, 2018. [6](#), [8](#)
- [72] Huiyu Wang, Yukun Zhu, Bradley Green, Hartwig Adam, Alan L. Yuille, and Liang-Chieh Chen. Axial-deeplab: Stand-alone axial-attention for panoptic segmentation. In *ECCV*, 2020. [7](#), [8](#)
- [73] Yanwei Li, Lin Song, Yukang Chen, Zeming Li, Xiangyu Zhang, Xingang Wang, and Jian Sun. Learning dynamic routing for semantic segmentation. In *CVPR*, 2020. [7](#)
- [74] Gerhard Neuhold, Tobias Ollmann, Samuel Rota Bulò, and Peter Kotschieder. The mapillary vistas dataset for semantic understanding of street scenes. In *ICCV*, 2017. [9](#)
- [75] Christoph Kamann and Carsten Rother. Benchmarking the robustness of semantic segmentation models. In *CVPR*, 2020. [9](#)

Checklist

1. For all authors...
 - (a) Do the main claims made in the abstract and introduction accurately reflect the paper’s contributions and scope? [\[Yes\]](#)
 - (b) Did you describe the limitations of your work? [\[Yes\]](#) Please Section [5](#).
 - (c) Did you discuss any potential negative societal impacts of your work? [\[Yes\]](#) Please see Broader Impact.
 - (d) Have you read the ethics review guidelines and ensured that your paper conforms to them? [\[Yes\]](#)
2. If you are including theoretical results...
 - (a) Did you state the full set of assumptions of all theoretical results? [\[N/A\]](#)
 - (b) Did you include complete proofs of all theoretical results? [\[N/A\]](#)
3. If you ran experiments...
 - (a) Did you include the code, data, and instructions needed to reproduce the main experimental results (either in the supplemental material or as a URL)? [\[Yes\]](#)
 - (b) Did you specify all the training details (e.g., data splits, hyperparameters, how they were chosen)? [\[Yes\]](#)
 - (c) Did you report error bars (e.g., with respect to the random seed after running experiments multiple times)? [\[No\]](#) We observed quite stable mIoU results for semantic segmentation models.
 - (d) Did you include the total amount of compute and the type of resources used (e.g., type of GPUs, internal cluster, or cloud provider)? [\[Yes\]](#)

4. If you are using existing assets (e.g., code, data, models) or curating/releasing new assets...
 - (a) If your work uses existing assets, did you cite the creators? [Yes] Please see Section 4.
 - (b) Did you mention the license of the assets? [Yes] The data used in our work is open source and can be used for academic research.
 - (c) Did you include any new assets either in the supplemental material or as a URL? [Yes] We provide our code for this work in the supplemental material.
 - (d) Did you discuss whether and how consent was obtained from people whose data you're using/curating? [N/A] The data used in our work is open source and can be used for academic research.
 - (e) Did you discuss whether the data you are using/curating contains personally identifiable information or offensive content? [N/A] The data does not contain personally identifiable information or offensive content.
5. If you used crowdsourcing or conducted research with human subjects...
 - (a) Did you include the full text of instructions given to participants and screenshots, if applicable? [N/A]
 - (b) Did you describe any potential participant risks, with links to Institutional Review Board (IRB) approvals, if applicable? [N/A]
 - (c) Did you include the estimated hourly wage paid to participants and the total amount spent on participant compensation? [N/A]